Pharmaceutica Analytica Acta
ISSN: 2153-2435

Jana et al., Pharm Anal Acta 2015, 6:10
DOI: 10.4172/2153-2435.1000435

Research Article Open Access

Physical and Structural Characterization of Biofield Energy Treated Carbazole

Snehasis Jana[1]*, Mahendra Kumar Trivedi[1], Alice Branton[1], Dahryn Trivedi[1], Gopal Nayak[1] and Gunin Saikia[2]

[1]*Trivedi Global Inc., 10624 S Eastern Avenue Suite A-969, Henderson, NV 89052, USA*
[2]*Trivedi Science Research Laboratory Pvt. Ltd., Hall-A, Chinar Mega Mall, Chinar Fortune City, Hoshangabad Rd., Bhopal-462026, Madhya Pradesh, India*

Abstract

Carbazole is a class of phytochemical associated with cancer prevention. It attracted a significant interest in recent time for their usefulness in synthetic heterocyclic chemistry, analytical chemistry and pharmacology. The aim of the study was to evaluate the impact of biofield energy treatment on carbazole by various analytical methods. The study was performed in two groups i.e. control and treatment. The treatment group was subjected to Mr. Trivedi's biofield treatment. Subsequently, both the samples were characterized with respect to physical and structural properties using X-ray diffraction (XRD), differential scanning calorimetry (DSC), thermogravimetric analysis (TGA), Fourier transform infrared (FT-IR), gas chromatography-mass spectrometry (GC-MS), laser particle size analyzer, and surface area analyzer. The XRD study revealed that the crystallite size of treated carbazole was decreased significantly with 37.5% as compared to the control. In addition, the intensity of XRD peaks was slightly decreased as compared to the control. The latent heat of fusion (ΔH) of treated carbazole was substantially increased by 253.6% as compared to the control. Maximum degradation temperature (T_{max}) of treated carbazole was increased by 41.46°C as compared to the control (211.93°C to 253.39°C). FT-IR spectra showed similar stretching frequencies in both control and treated carbazole samples. GC-MS data revealed that isotopic abundance ratio of either $^{13}C/^{12}C$ or $^{15}N/^{14}N$ or $^{2}H/^{1}H$ (PM+1/PM) of treated carbazole was significantly increased up to 278.59%. Particle size analysis showed substantial decrease in average particle size (d_{50}) and d_{90} of the treated carbazole by 25.24% and 4.31%, respectively as compared to the control. The surface area analysis exhibited an increase in the surface area of treated sample by 4.8% as compared to the control. Overall, the experimental results suggest that biofield energy treatment has significant effect on physical, spectral and thermal properties of carbazole.

Keywords: Carbazole; Biofield energy treatment; Fourier transform infrared; Differential scanning calorimetry; Thermogravimetric analysis; X-ray diffraction; Gas chromatography-mass spectrometry

Abbreviations: XRD: X-Ray Diffraction; FT-IR: Fourier Transform Infrared; GC-MS: Gas Chromatography-Mass Spectrometry; DSC: Differential Scanning Calorimetry; TGA: Thermogravimetric Analysis; PM: Primary Molecule (m/z = 167 For Carbazole); PM+1: Represents Isotopic Molecule (m/z = 168)

Introduction

Carbazole is a nitrogen containing heterocycle, which was found in nature as alkaloids and in crude oils (0.3%). Out of 0.3% in crude oil, a major fraction, about 70-75% is comprised of heterocycles, carbazole and indole [1]. The preliminary research had conducted by Stanford Medicine, they conclude that the compounds present in food called phytochemicals; (carbazole and indole class of phytochemicals) which can decrease the risk of developing diseases such as hypertension, diabetes, and cancer [2]. Carbazole and indole have received significant attention in compounds which are active against cancer, and cardiovascular disorders [3,4], that exhibit antioxidant, antidiabetic, antimitotic, and antimicrobial activities [5-8]. Furthermore, carbazole derivatives also play a significant role as an active material in the organic light emitting diodes for blue light emission and organic field-effect transistors (OFET) [9,10]. Due to their wide range of synthetic applications, in the development of pharmaceutical and organic semiconductors, chemical or physical stability is the main concern and utmost criteria. The stability could be enhanced by Mr. Trivedi's biofield energy treatment which is already known to alter the physical, and structural properties of various living and non-living substances [11]. The biofield, which surrounds the human body, and can be harnessed from the Universe. It has been applied on materials by experts in a controlled way to make the changes [12]. This phenomenon is experimentally demonstrated by researchers and biofield can be measured using medical technologies such as electromyography, electrocardiography, and electroencephalogram [13]. National Center for Complementary and Alternative Medicine (NCCAM) has recommended the uses of alternative Complementary and Alternative Medicine (CAM) therapies in the healthcare sector and about 36% of Americans regularly use some form of CAM [14]. Mr. Trivedi has the ability to harness the energy from the universe and can transmit the energy into any object, living or nonliving things [15]. Mr. Trivedi's unique biofield treatment is also known as The Trivedi Effect® which has been applied in various research fields including microbiology research [17], agriculture research [18], and biotechnology research [19]. Thus, in this study, Mr. Trivedi's biofield energy treatment was applied on carbazole to see the impact with respect to their physical, thermal and spectral properties.

***Corresponding author:** Snehasis Jana, Trivedi Global Inc., 10624 S Eastern Avenue Suite A-969, Henderson, NV 89052, USA, Tel: +91-755-6660006; E-mail: publication@trivedisrl.com

Received September 22, 2015; **Accepted** October 20, 2015; **Published** October 23, 2015

Citation: Jana S, Trivedi MK, Branton A, Trivedi D, Nayak G, et al. (2015) Physical and Structural Characterization of Biofield Energy Treated Carbazole. Pharm Anal Acta 6: 435. doi:10.4172/21532435.1000435

Experimental

Materials

Carbazole was procured from Sisco Research Laboratories (SRL), India.

Biofield energy treatment modalities

Carbazole was taken in this experiment for biofield energy treatment. The compound was divided into two parts named as control and treated. No treatment was given to the control set. The treated group was handed over to Mr. Trivedi for biofield energy treatment in sealed pack under standard laboratory conditions. Mr. Trivedi provided the treatment through his energy transmission process to the treated group without touching the sample. After treatment, the treated samples were stored at standard laboratory conditions for GC-MS analysis as per the standard operating protocol. The control and treated samples were characterized using Gas chromatography-mass spectrometry (GC-MS). The experimental results in treated groups were analyzed and compared with the control set.

Percent changes in treated sample with respect to control were calculated using the following equation:

%Change = [Treated-Control]/Control×100

X-ray diffraction (XRD) study

XRD analysis of carbazole was carried out on Phillips, Holland PW 1710 X-ray diffractometer system, with radiation of wavelength 1.54056 Å. The crystallite size (G) was calculated by using formula: $G = k\lambda/(b\cos\theta)$. Here, λ is the wavelength of radiation, b is full-width half maximum (FWHM) of peaks and k is the equipment constant (=0.94).

Differential scanning calorimetry (DSC) study

The DSC thermogram of carbazole was acquired by using Perkin Elmer/Pyris-1, USA at flow rate of 5 mL/min using closed aluminum pan. Melting temperature and latent heat of fusion were obtained from the DSC curve.

Thermogravimetric analysis (TGA)/ derivative thermogravimetry (DTG)

TGA/DTG results were obtained by using Mettler Toledo simultaneous thermogravimetric analyzer at a heating rate of 5°C/min from room temperature to 400°C under air atmosphere.

FT-IR spectroscopic characterization

FT-IR characterization was done with Shimadzu Fourier transform infrared spectrometer (Japan) with frequency range of 500-4000 cm^{-1}. Carbazole was run as pressed disks using KBr as the diluent.

GC-MS analysis

The gas chromatography-mass spectrometry (GC-MS) analysis was performed on Perkin Elmer/auto system XL with Turbo Mass, USA, having detection limit up to 1 picogram. The GC-MS data was obtained in the form of % abundance vs. mass to charge ratio (m/z), which is known as mass spectrum. The isotopic ratio of PM+1/PM was expressed by its deviation in treated samples as compared to the control.

Particle size analysis

Particle size distribution of control and treated samples were analyzed by using Sympetac Helos-BF laser particle size analyzer with a detection range of 0.1 to 875 µm. Average particle size d_{50} and d_{99} (size exhibited by 99% of powder particles) were computed from laser diffraction data table.

Surface area analysis

The surface area was measured by Smart SORB 90, the Brunauer–Emmett–Teller (BET) surface area analyzer.

Results and Discussion

X-ray diffraction studies

XRD study was conducted on both control and treated samples of carbazole and diffractograms are shown in Figure 1. Both control and treated carbazole samples exhibited very sharp and intense peaks of intensity 6200 a.u. and 4900 a.u., in their respective X-ray diffractograms. The control carbazole exhibited the XRD peaks at 2θ equal to 18.52, 27.95, 36.4, 37.6, 47.01, and 47.49. However, the XRD diffractogram of treated carbazole showed the XRD peaks at 2θ equal to 18.49, 27.89, 27.99, 37.49, 37.61, and 47, with decreased intensity

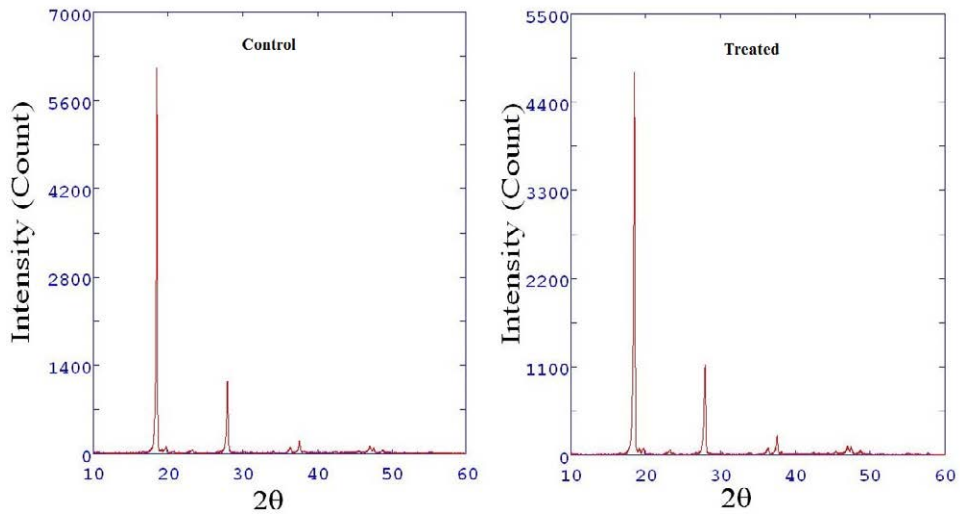

Figure 1: X-ray diffractograms of control and treated samples of carbazole.

Carbazole	2θ	FWHM of peak intensity 100%	Crystallite size 'G' x 10^{-9} m	Percent change in 'G' wrt control
Control	18.52, 27.95, 36.4, 37.6, 47.01, 47.49	0.12	85.83	
Treated	18.49, 27.89, 27.99, 37.49, 37.61, 47	0.18	52.40	-37.50

FWHM: full width half maximum, wrt: with respect to.

Table 1: XRD analysis of control and treated carbazole.

as compared to the control (Table 1). Literature report showed that the single crystals of carbazole are orthorhombic with four molecules in a unit cell [20]. The crystallite size was calculated using Scherrer formulae and found decreased after biofield treatment by 37.50% in the treated carbazole [21]. Moreover, it was reported that crystallite size and surface area are inversely proportional to each other [22]. The solubility profile of carbazole may alter after biofield treatment, as the crystallite size of the compound decreased which may increase the surface area and hence increase the solubility.

DSC analysis

The DSC curve of control and treated samples of carbazole are shown in Figure 2. The latent heat of fusion (ΔH) was increased in the treated carbazole from 56.22 to 198.60 J/g (~253%). It might be possible that biofield energy favoring a strong π-π interaction of carbazole moiety in solid state. As the hydrogen bond such as N-H…N is not possible to form in the crystal due to the position (H atom is on the plane of the molecule) and hybridization of N atom [20]. A higher melting point was observed in the treated carbazole (247.53 °C) as compared to the control sample (245.54 °C), (Table 2). This result showed that treated carbazole sample needed more energy in the form of ΔH to undergo the process of melting at a higher temperature. It is hypothesized that the biofield energy might increase the intermolecular force in treated carbazole molecules, which possibly increase the melting point and latent heat of fusion.

TGA/DTG analysis

The TGA thermogram of both control and treated samples of carbazole are shown in Figure 3(a) and 3(b), respectively. TGA curve showed that the control and treated samples were degraded in two steps. For first step degradation, in control sample, the onset temperature was at 179.72°C and endset at 230°C. However, in treated sample, onset temperature was observed at 224.18°C and endset at 275.55°C. In this process, the control sample lost 29.6% of its initial weight, whereas treated sample lost 44.20% of its initial weight. For the second step degradation, in control sample, the onset temperature was found at 258°C and endset at 336°C, while treated sample showed the onset at 282.59°C and endset at 308.75°C. In this process, control sample lost its weight of 57.46%, whereas treated sample lost 1.14% of its initial weight. The DTG thermogram showed the T_{max} corresponding to first and second step degradation as 211.93°C and 298.91°C, respectively in control, which was changed to 253.39°C and 295.50°C, respectively in treated sample. It indicated that T_{max} for the first step was increased in treated sample as compared to the control. Thus, the increase in melting temperature and maximum degradation temperature of treated carbazole can be related to increase in thermal stability. The overall increases in thermal stability of treated sample might be advantageous to be used as a core moiety (pharmacophore) in medicine and synthetic conducting polymers.

FT-IR spectroscopic analysis

FTIR spectra of control and treated samples of carbazole are presented in Figure 4. The FTIR spectra showed the secondary amine N-H stretching frequency at 3419 cm^{-1} for control and treated samples of carbazole. The IR spectra of both control and treated carbazole samples showed C-N stretching at 1450 cm^{-1} and out of plane NH bending at 727 cm^{-1}. Furthermore, the C-H deformation bends were assigned to the peaks at 1327 cm^{-1} in both control and treated samples of carbazole. The C-H aromatic stretching frequency was observed at 3051 cm^{-1} for both control and treated samples of carbazole. N-C aromatic stretching frequency was observed at 1327 cm^{-1} in both the control and treated samples of carbazole. The spectra indicated that there was no alteration in the hydrogen bonding environment in both treated and control samples of carbazole. The FT-IR results did not show any major shift of frequencies in both aromatic and functional group region (N-H, N-C, and C-H stretching frequency). The FTIR spectral data is well matched with the literature data [23].

GC-MS spectrometry

The treated sample of carbazole was divided into four parts as T1, T2, T3, and T4. The mass spectrum of control and treated samples of carbazole are shown in Figure 5(a) and 5(b). Mass spectra showed the PM (primary molecule) peak at m/z = 167 in control and all the treated

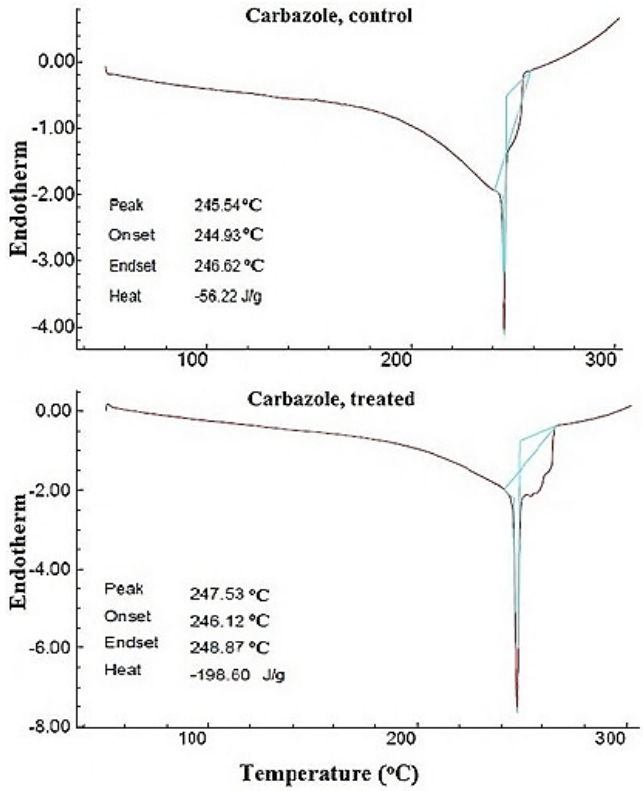

Figure 2: DSC plots of control and treated carbazole.

Parameter		Carbazole
Latent heat of fusion ΔH (J/G)	Control	Treated
	56.22	198.60
Melting point (°C)	245.54	247.53

Table 2: DSC analysis of control and treated carbazole.

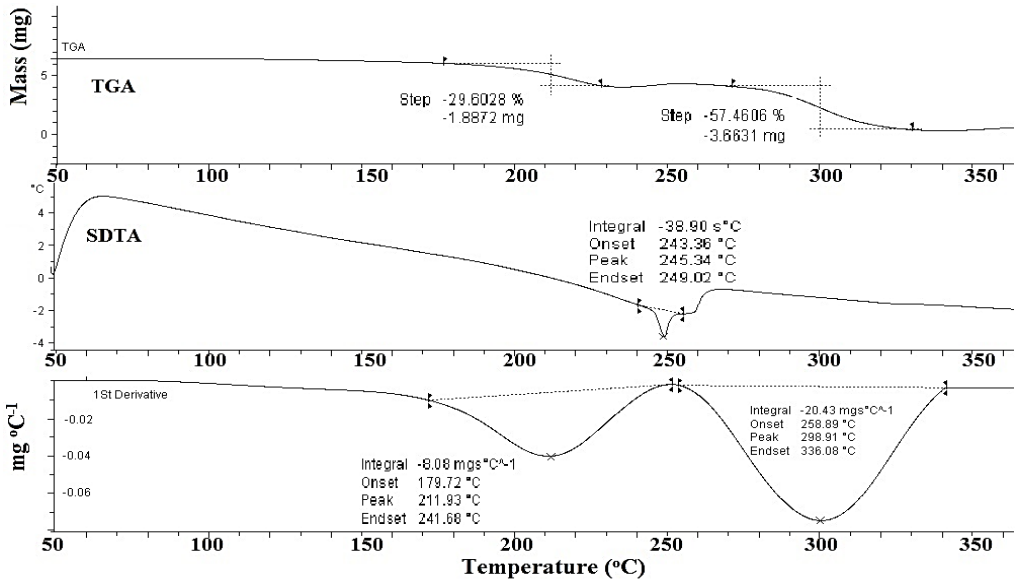

Figure 3a: TGA thermogram of control sample of carbazole.

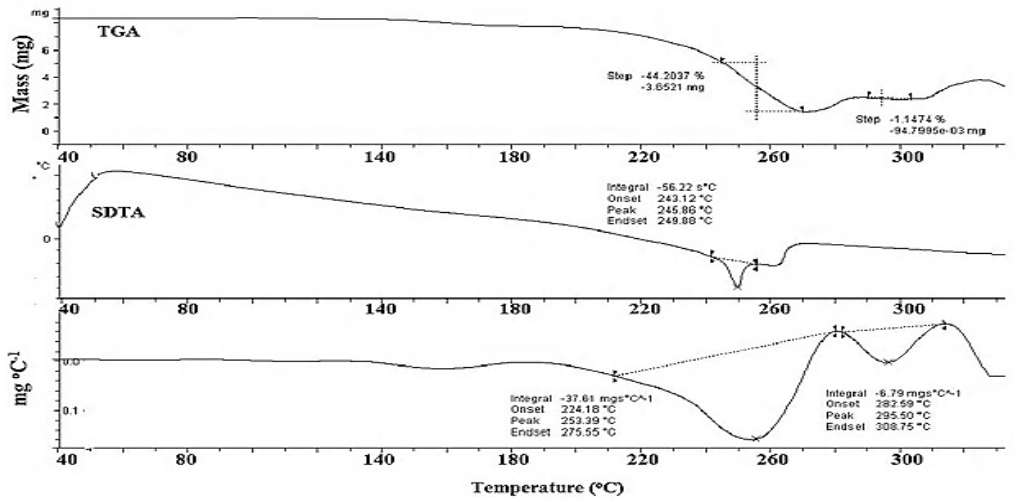

Figure 3b: TGA thermogram of treated sample of carbazole.

samples of carbazole. The intensity ratio of PM+1 (i.e. m/z = 168) and PM (i.e. m/z = 167) peaks are presented in Table 3. There were three major peaks observed in control sample i.e. at m/z = 167, 139 and 84 due to carbazole and its degraded products. The degradation of carbazole, corresponded to the following ions: $C_{10}H_5N^+$ and $C_5H_{10}N^+$ respectively, were well matched with the previously reported GC-MS data [24]. The treated carbazole samples (T1-T4) were fragmented in a different way as compared to the control. For instance, peaks at m/z = 113, 63, 39, and 28 were observed in T1 to T4 due to PM fragmentation of treated carbazole to $C_7H_{15}N^+$, $C_5H_3^+$ $C_3H_3^+$ and $C_2H_2^+$ radicals respectively. Isotopic abundance ratio of $^{13}C/^{12}C$ or $^{15}N/^{14}N$ or $^{2}H/^{1}H$ (PM+1)/PM in carbazole was calculated and presented in Figure 6. It showed that the isotopic ratio of (PM+1)/PM in carbazole was significantly increased by 278.59% in sample T4, while it was decreased by 26.26% in treated, T1 sample as compared to the control. The biofield treatment may have altered the isotopic abundance ratio of (PM+1)/PM of treated carbazole from the control sample. Furthermore, it is assumed that higher isotopic ratio of (PM+1)/PM, might have increased the stability of the compound due to the increased μ (reduced mass) and binding energy in molecules in heavier isotopic compound. This higher binding energy may lead to increase the bond strength for treated carbazole and reverse might happen in treated T1 [25]. Thus, GC-MS data suggested that biofield treatment has significantly altered the isotopic ratio of $^{13}C/^{12}C$ or $^{15}N/^{14}N$ or $^{2}H/^{1}H$ (PM+1)/PM to 278.59%, in treated carbazole molecule. The lattice parameters of two chemically identical crystals formed by different isotopes do not correspond to the same value which may be reflected in the increased melting and degradation temperature of the treated molecule [26,27].

Particle size analysis

The particle size of control and treated carbazole is computed from the particle size distribution graph. The average particle size of d_{50} and

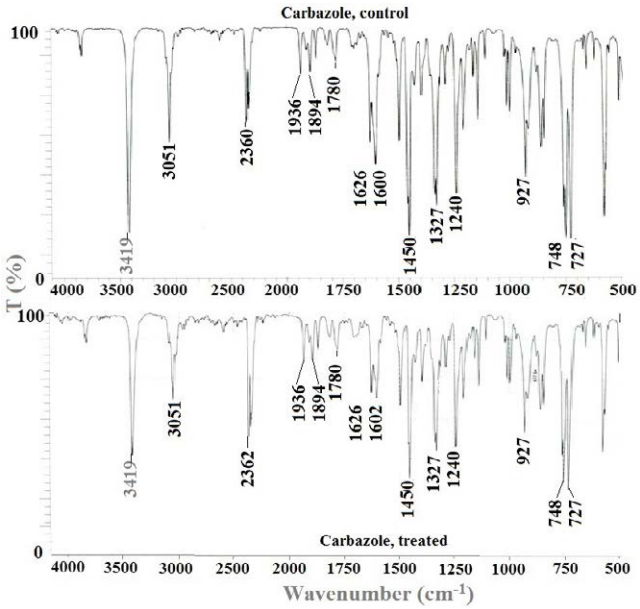

Figure 4: FT-IR spectra of control and treated samples of carbazole.

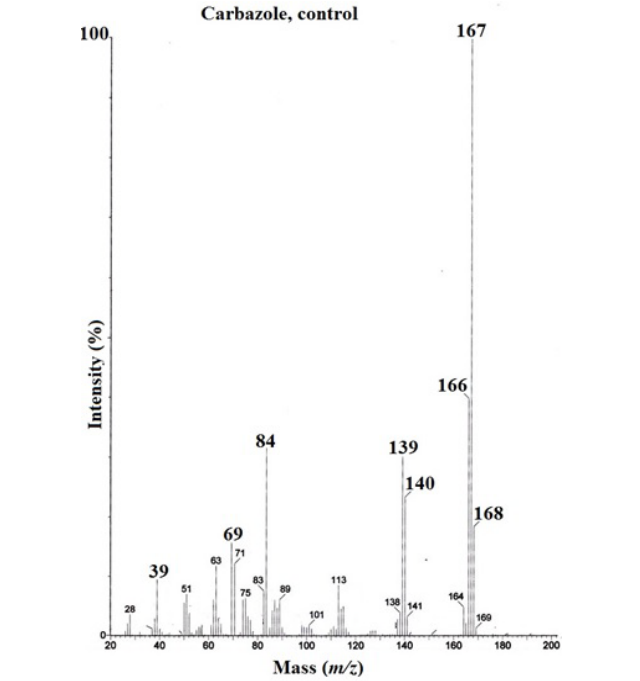

Figure 5a: GC-Mass spectrum of control sample of carbazole.

d_{90} of the particles are shown in Table 4. The d_{50} of control carbazole was 287.71 µm and it was decreased substantially to 215.08 µm in the treated sample. Whereas, the d_{90} of the control sample was 535.23 µm and it was decreased to 512.12 µm in treated sample. The result showed significant decrease in d_{50} and d_{90} by 25.24 and 4.31%, respectively in the treated carbazole with respect to control sample. This distinct reduction in particle size of treated compound due to the biofield energy treatment and it is supported by decrease in crystallite size in the XRD results. It is assumed that the energy treatment might fracture the internal boundaries of particles and that may result into smaller particle size [28].

Surface area analysis

The surface area analysis was conducted using BET method and results are presented in Figure 7. The control sample showed a surface area of 0.46 m^2/g and it was increased to 0.48 m^2/g in treated samples of carbazole. The result showed increase in surface area of treated sample by 4.80% with respect to the control. Crystallite size and particle size are inversely proportional to the surface area of the compound. Thus, the decrease in particle size led to increase the surface area of treated sample.

Conclusions

In summary, the crystallite size was significantly decreased by 37.50% in treated carbazole as compared to the control. In addition, the decrease in the intensity of the diffractogram in treated samples may be due to the decrease in crystallinity. The melting point and latent heat of fusion were substantially increased by ~2°C and 142 J/g, respectively

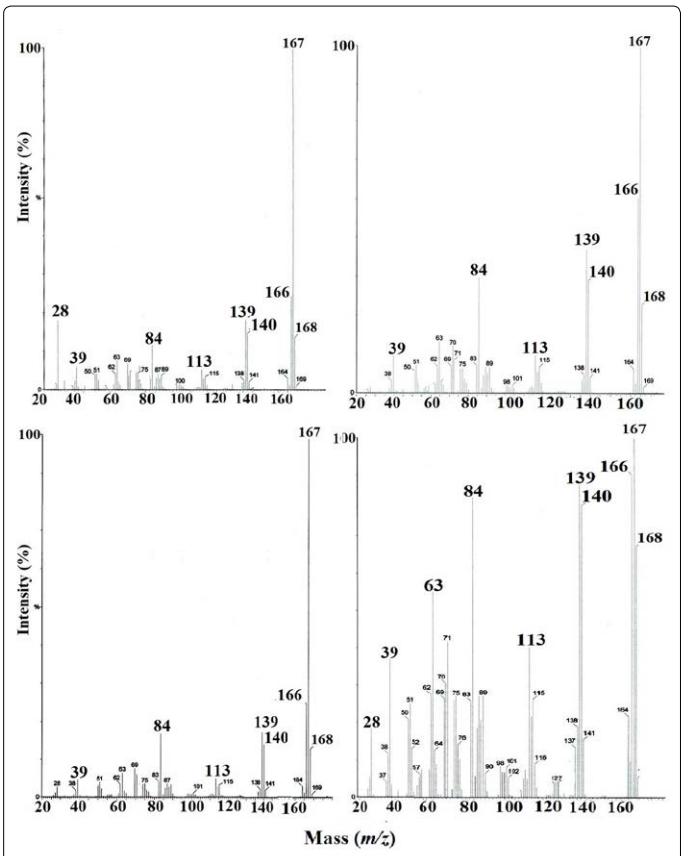

Figure 5b: GC-MS spectra of treated (T1, T2, T3 and T4) samples of carbazole.

Parameter	Control	Treated			
		T1	T2	T3	T4
Peak Intensity at m/z= (PM)	100	100	100	100	100
Peak Intensity at m/z= (PM+1)	18.36	13.54	22.70	12.81	69.51
Percent Change of Isotopic abundance in (PM+1)/PM		-26.25	23.63	-30.22	278.59

Table 3: GC-MS isotopic abundance analysis result of carbazole.

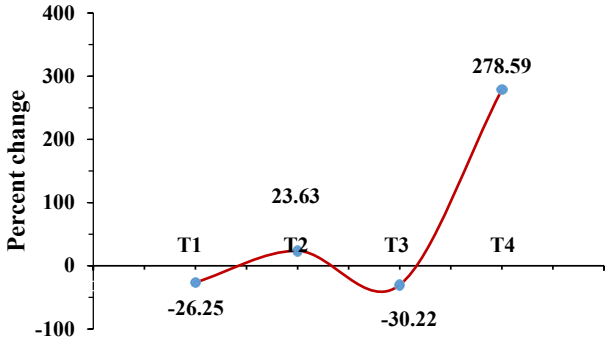

Figure 6: Percent change in isotopic abundance ratio of (PM+1)/PM in treated samples of carbazole.

Particle Size	Control (µm)	Treated (µm)
d_{50}	287.71	215.08
d_{90}	535.23	512.12

Table 4: The average particle size of control and treated carbazole.

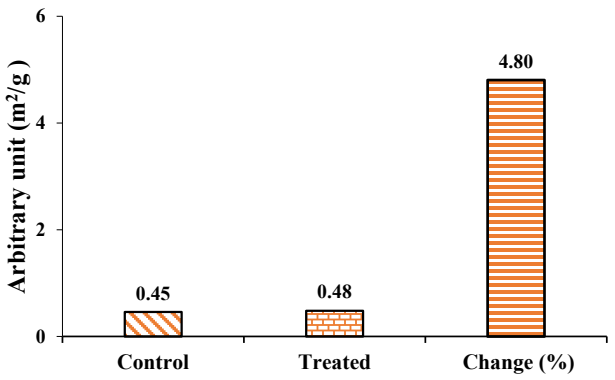

Figure 7: Surface area analysis of control and treated carbazole sample.

in treated samples as compared to the control. Moreover, maximum degradation temperature (T_{max}) was increased by 41.46°C that indicated the enhanced thermal stability of the biofield treated carbazole. The GC-MS data revealed that isotopic abundance ratio of $^{13}C/^{12}C$ or $^{15}N/^{14}N$ or $^{2}H/^{1}H$ (PM+1)/PM of treated carbazole was significantly increased up to 278.59% of T4 sample as compared to the control. It is assumed that due to high isotopic abundance ratio of (PM+1)/PM of treated (T4) carbazole, with higher binding energy may lead to higher chemical stability than the control. This is well corroborated with the particle size and surface area analysis of the carbazole sample. It is assumed that the enhancement in thermal stability of carbazole could be more useful as a building block in various pharmaceutical products and conducting polymers which ultimately affect the shelf-life and efficacy of the product.

Acknowledgements

The authors would like to acknowledge the whole team of MGV Pharmacy College, Nashik and Indian Rubber Manufacturers Research Association (IRMRA), Thane for providing the instrumental facility. We would also like to thank Trivedi Science™, Trivedi Master Wellness™ and Trivedi Testimonials for their support during the work.

References

1. Riddle RR, Gibbs PR, Willson RC, Benedik MJ (2003) Recombinant carbazole-degrading strains of enhanced petroleum processing. J Ind Microbiol Biotechnol 30: 6-12.
2. Janet Renee (2014) Which Foods Are High in Indoles?.
3. Lemster T, Pindur U, Lenglet G, Depauw S, Dassi C, et al. (2009) Photochemical electrocyclisation of 3-vinylindoles to pyrido[2,3-a]-,pyrido[4,3-a]-and thieno[2,3-a]-carbazoles: Design, synthesis, DNA binding and antitumor cell cytotoxicity. Eur J Med Chem 44: 3235-3252.
4. Laronze M, Boisbrun M, Leonce S, Pfeiffer B, Renard P, et al. (2005) Synthesis and anticancer activity of new pyrrolocarbazoles and pyrrolo-beta-carbolines. Bioorg Med Chem 13: 2263-2283.
5. Sauerberg P, Pettersson I, Jeppesen L, Bury PS, Mogensen JP, et al. (2002) Novel tricyclic-alpha-alkyloxy phenyl propionic acids: Dual PPAR alpha/gamma agonists with hypolipidemic and antidiabetic activity. J Med Chem 45: 789-804.
6. Jayakumar SV, Ganesh SMK (2012) The efficacy of aqueous methanolic extract of Murraya koenigi (L.) Spreng in alloxan induced diabetic albino rats. Asian J Plant Sci Res 2: 263-268.
7. Barta TE, Barabasz AF, Foley BE, Geng L, Hall SE, et al. (2009) Novel carbazole and acyl-indole antimitotics. Bioorg Med Chem Lett 19: 3078-3080.
8. Zhang FF, Gan LL, Zhou CH (2010) Synthesis, antibacterial and antifungal activities of some carbazole derivatives. Bioorg Med Chem Lett 20: 1881-1884.
9. Freeman AW, Urvoy M, Criswell ME (2005) Triphenylphosphine-mediated reductive cyclization of 2-nitrobiphenyls: A practical and convenient synthesis of carbazoles. J Org Chem 70: 5014-5019.
10. Kapil K, Kumar N, Pathak D (2012) Synthesis of some newer carbazole derivatives and evaluation for their pharmacological activity. Der Pharmacia Sinica 3: 470-478.
11. Trivedi MK, Patil S, Shettigar H, Bairwa K, Jana S (2015) Phenotypic and biotypic characterization of Klebsiella oxytoca: An impact of biofield treatment. J Microb Biochem Technol 7: 203-206.
12. Rubik B (2002) The biofield hypothesis: Its biophysical basis and role in medicine. J Altern Complement Med 8: 703-717.
13. Rivera-Ruiz M, Cajavilca C, Varon J (2008) Einthoven's string galvanometer: The first electrocardiograph. Tex Heart Inst J 35: 174-178.
14. Barnes PM, Powell-Griner E, McFann K, Nahin RL (2004) Complementary and alternative medicine use among adults: United States, 2002. Adv Data 343: 1-19.
15. Trivedi MK, Patil S, Tallapragada RMR (2015) Effect of biofield treatment on the physical and thermal characteristics of aluminium powders. Ind Eng Manage 4: 151.
16. Maxwell JC (1865) A dynamical theory of the electromagnetic field. Phil Trans R Soc Lond 155: 459-512.
17. Trivedi MK, Patil S, Shettigar H, Gangwar M, Jana S (2015) Antimicrobial sensitivity pattern of Pseudomonas fluorescens after biofield treatment. J Infect Dis Ther 3: 222.
18. Sances F, Flora E, Patil S, Spence A, Shinde V (2013) Impact of biofield treatment on ginseng and organic blueberry yield. Agrivita J Agric Sci 35.
19. Patil SA, Nayak GB, Barve SS, Tembe RP, Khan RR (2012) Impact of biofield treatment on growth and anatomical characteristics of Pogostemon cablin (Benth.). Biotechnology 11: 154-162.
20. Kurahashi M, Fukuyo M, Shimada A, Furusaki A, Nitta I (1969) The crystal and molecular structure of carbazole. Bull Chem Soc Japan 42: 2174-2179.
21. Langford JI, Wilson AJC (1978) Scherrer after sixty years: A survey and some new results in the determination of crystallite size. J Appl Cryst 11: 102-113.
22. Behnajady MA, Aalamdari ME, Modirshahla N (2013) Investigation of the effect of heat treatment process on characteristics and photocatalytic activity of TiO_2-UV100 nanoparticles. Environ Prot Eng 39: 33-46.
23. http://webbook.nist.gov/cgi/cbook.cgi?ID=C86748&Mask=80#IR-Spec
24. http://webbook.nist.gov/cgi/cbook.cgi?ID=C86748&Mask=200#Mass-Spec
25. Rieley G (1994) Derivatization of organic-compounds prior to gas-chromatographic combustion-isotope ratio mass-spectrometric analysis: Identification of isotope fractionation processes. Analyst 119: 915-919.

26. Plekhanov VG (2001) Isotope Effects in Solid State Physics (1st edn) Academic Press, San Diego CA USA.

27. Haller EE (1995) Isotopically engineered semiconductors. J Appl Phys 77: 2857-2878.

28. Trivedi MK, Patil S, Tallapragada RM (2014) Atomic, Crystalline and Powder Characteristics of Treated Zirconia and Silica Powders. J Material Sci Eng 3: 144.